Available online at www.sciencedirect.com
ScienceDirect
Polyhedron 26 (2007) 2655–2662
POLYHEDRON
www.elsevier.com/locate/poly

Mechanistic studies on the Pd–Cl cleavage of dichloro-[1-alkyl-2-(naphthylazo)imidazole]palladium(II) complexes by 8-quinolinol

Pradip Kumar Ghosh, Sushanta Saha, Ambikesh Mahapatra *

Department of Chemistry, Jadavpur University, Kolkata 700 032, India

Received 6 December 2006; accepted 10 January 2007
Available online 30 January 2007

Abstract

8-Quinolinol (HQ) reacts with [Pd(α-/β-NaiR)Cl_2] [α-/β-NaiR = 1-alkyl-2-(naphthyl-α-/β-azo)imidazole] in acetonitrile (MeCN) solution to give [Pd(α-/β-NaiR)(Q)](ClO_4). The products are characterized by spectroscopic techniques (FT-IR, UV–Vis, NMR). The reaction kinetics show a first order dependence of rate on each of the concentration of the metal complex and HQ. Addition of LiCl to the reaction retarded the rate of reaction and has proved the cleavage of the Pd–Cl bond as the rate-determining step. Thermodynamic parameters ($\Delta^{\ddagger}H^{\circ}$ and $\Delta^{\ddagger}S^{\circ}$) are determined from variable temperature kinetic studies. The magnitude of the second order rate constant, k_2, increases as in the order: Pd(NaiEt)Cl_2 < Pd(NaiMe)Cl_2 < Pd(NaiBz)Cl_2 as well as Pd(β-NaiR)Cl_2 < Pd(α-NaiR)Cl_2.

Keywords: Palladium(II); Substitution; Naphthylazoimidazole; 8-Quinolinol; Pd–Cl cleavage; π-Acidity

1. Introduction

The reaction of DNA bases with platinum/palladium complexes of chelating *N*,*N*′ donors having a *cis*-MCl_2 configuration constitutes a model system which may allow for exploration of the mechanism of the anti-tumor activity of *cis*-platin [1–9]. Both palladium(II) and platinum(II) ions form diamagnetic planar complexes and strongly prefer nitrogen and oxygen donor atoms [10]. Due to very low reacting equilibrium constants for Pt(II) complexes and their kinetic inertness compared to Pd(II) complexes ($\sim 10^5$ times slow) [11,12], the reactions are uncertain in terms of mechanistic studies. Structurally analogous Pd(II) complexes may be used to find out the mechanism of interaction of DNA bases with Pt(II)-anticancer agents. Arylazoimidazoles are bidentate *N*,*N*′-chelators and form M(*N*,*N*′)Cl_2 complexes having a *cis*-MCl_2 configuration. The kinetics and mechanism of the substitution reactions involving Pd(II) complexes of aryl-azo heterocycles with adenine [13], cytosine [14], 2-mercapto-pyridine [15], 2-amino-pyrimidine [16], picolinic acid [17] and 8-quinolinol [18] have been reported. We are intending to incorporate higher steric crowding around the target metal center by using different ligands with a basic azoimine chelating mode (–N=N–C=N–), which will open an avenue to find out mechanistic aspects of the nucleophilic interaction with the metal center under different local environments. Naphthylazoimidazoles (**ii**) are chemical analogues to phenylazoimidazoles (**i**), but with a higher degree of steric crowding and electron donating ability. Herein we present the kinetic and mechanistic studies of the reaction of 8-quinolinol (HQ) with Pd(α/β-NaiR)Cl_2.

* Corresponding author. Tel.: +91 33 2432 4586; fax: +91 33 2414 6584.
E-mail addresses: ambikesh_ju@yahoo.com, amahapatra@chemistry.jdvu.ac.in (A. Mahapatra).

0277-5387/$ - see front matter © 2007 Elsevier Ltd. All rights reserved.
doi:10.1016/j.poly.2007.01.022

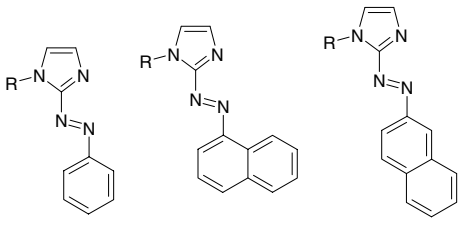

Phenylazoimidazole (**i**) Naphthylazoimidazole (**ii**)

2. Experimental

2.1. Reagents/materials

The complexes were prepared by a reported procedure [19,20]. 8-Quinolinol (SRL, Mumbai) was purified by recrystallization from a hot ethanol solution. Acetonitrile (MeCN) was purified by a known procedure [21,22]. All kinetic and spectroscopic measurements were recorded on an Agilent 8453E UV–visible Spectroscopy System. Quartz cells (1.0 cm path length) from Hellma were used. IR spectra (KBr pellet) were recorded on a FT-IR spectrophotometer Spectrum RX1, Perkin–Elmer. ^{1}H NMR spectra were drawn from a 300 MHz Bruker NMR instrument in CD_3CN using TMS as an internal standard. Microanalyses were carried out on a Perkin–Elmer 2400 CHN elemental analyzer. The specific conductance was measured on a JENCONS 4010 Conductivity Meter. The pH was measured on a SYSTRONICS 361 Digital pH meter. Rate constants and standard deviations were calculated by linear regression using a PC-based program, Microcal-origin version Origin-6.1.

2.1.1. Kinetic measurements

For kinetic measurements, stock solutions of the complexes (*ca.* 10^{-3} mol dm^{-3}) and of 8-quinolinol (HQ) (*ca.* 10^{-2} mol dm^{-3}) were prepared in dry MeCN. Solutions of different concentrations were prepared by quantitative dilution of stock solutions using dry MeCN. All experiments were performed at 298 K (unless otherwise mentioned) by mixing required volumes of the thermostated reactants and transferring the mixture to the absorption cell (1.0 cm length). On addition of 8-quinolinol (HQ) to the solution of Pd(NaiR)Cl_2 in MeCN, the orange solution changed to yellow-orange. The influence of the addition of 8-quinolinol on the spectra of Pd(α-NaiR)Cl_2 is shown in the Fig. 1. The change proceeds through a single isobestic point at *ca.* 472 nm. The decrease in absorbance of the reaction mixture was recorded automatically at *ca.* 500 nm as a function of time (s). A_∞ was measured after ~24 h of mixing, when the absorbance became constant. In all experiments, the initial molar concentration of HQ, $[HQ]_0$, was kept at least ten times in excess so as to maintain a pseudo-first-order kinetic condition. Pseudo-first-order rate constants, k_{obs}, were obtained from the plots of $(A_t - A_\infty)$ versus time (s) (Fig. 2) where A_t = absorbance of the reaction mixture at time t (s) after mixing of the HQ solution and A_∞ = absorbance of same reaction mixture after completion of the reaction.

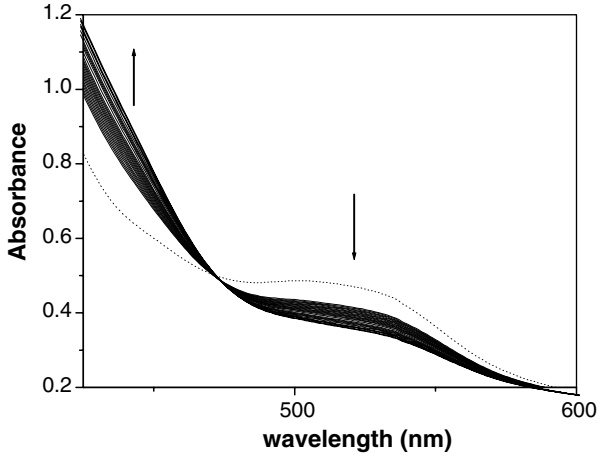

Fig. 1. Spectra of Pd(α-NaiMe)Cl_2in MeCN and a reaction mixture of Pd(α-NaiMe)Cl_2 and HQ in MeCN solution at 298 K. The arrows indicate the decrease and increase of band intensities as the reaction proceeds.

2.2. Synthesis of [Pd(α-/β-NaiR)(Q)](ClO$_4$) (α-NaiR, **3**; β-NaiR, **4**)

A representative synthesis of [Pd(α-NaiMe)(Q)](ClO_4) (**3a**) is given below.

To a MeCN solution of the complex Pd(α-NaiMe)Cl_2 (0.025 g, 6.05×10^{-2} mmol), HQ (0.026 g, 18.15×10^{-2} mmol) was added and the orange colored solution was stirred for about 24 h. It was filtered and allowed to evaporate to dryness at room temperature. The mass was then dissolved in MeOH, and $NaClO_4$ (aq) (1 g) was added to it. The brown precipitate that formed was filtered and washed

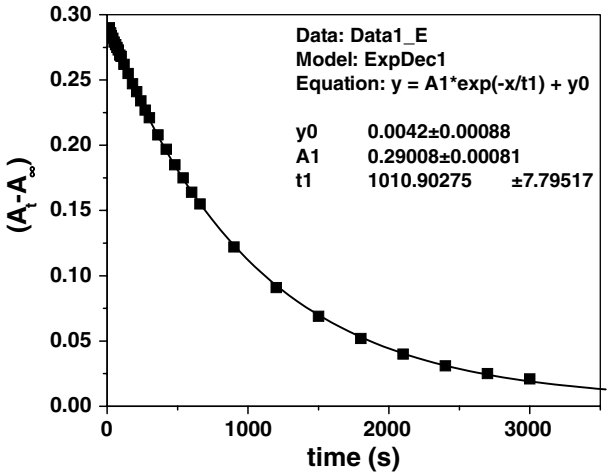

Fig. 2. Plot of $(A_t - A_\infty)$ vs. time (s) for the reaction: [Pd(α-NaiMe)Cl_2]$_0 = 1.09 \times 10^{-4}$ mol dm^{-3}, $[HQ]_0 = 3 \times 10^{-3}$ mol dm^{-3} and temperature = 298 K.

with water. The dried product was then chromatographed over silica gel and MeCN eluted an orange band. Yield: 0.023 g (64.7%).

All other complexes were prepared by the same procedure and the yields varied within 60–70%.

Microanalytical data of the complexes are as follows: For [Pd(α-NaiMe)(Q)][ClO_4) (**3a**): *Anal.* Found: C, 47.00; H, 3.02; N, 11.79%. Calc. for $C_{23}H_{18}O_5N_5PdCl$: C, 47.10; H, 3.07; N, 11.95. For [Pd(α-NaiEt)(Q)][ClO_4) (**3b**) *Anal.* Found: C, 48.08; H, 3.30; N,11.71%. Calc. for $C_{24}H_{20}O_5N_5PdCl$: C, 48.00; H, 3.33; N, 11.67. For [Pd(α-NaiBz)(Q)][ClO_4)(**3c**) *Anal.* Found: C, 52.72; H, 3.35; N, 11.11%. Calc. for $C_{29}H_{22}O_5N_5PdCl$: C, 52.58; H, 3.32; N, 11.04. For [Pd(β-NaiMe)(Q)][ClO_4) (**4a**) *Anal.* Found: C, 47.18; H, 3.12; N, 11.66%. Calc. for $C_{23}H_{18}O_5N_5PdCl$: C, 47.10; H, 3.07; N, 11.95. For [Pd(β-NaiEt)(Q)][ClO_4) (**4b**) *Anal.* Found: C, 47.88; H, 3.28; N, 11.78%. Calc. for $C_{24}H_{20}O_5N_5PdCl$: C, 48.00; H, 3.33; N, 11.67. For [Pd(β-NaiBz)(Q)][ClO_4) (**4c**) *Anal.* Found: C, 52.50; H, 3.27; N, 10.86%. Calc. for $C_{29}H_{22}O_5N_5PdCl$: C, 52.58; H, 3.32; N, 10.58.

3. Results and discussion

3.1. Kinetics and mechanism

Two classes of naphthylazoimidazole complexes of palladium(II) have been used in this work. They are Pd(α-NaiR)Cl_2 (**1**) (α-NaiR = 1-alkyl-2-(naphthyl-α-azo)-imidazole) and Pd(β-NaiR)Cl_2 (**2**) (β-NaiR = 1-alkyl-2-(naphthyl-β-azo)imidazole) [where R = Me (**a**)/Et (**b**)/Bz (**c**)]. The ligands belong to the unsymmetric bidentate *N*,*N*′-donor type and form dichloropalladium(II) complexes, here after we abbreviate the complexes as Pd(*N*,*N*′)Cl_2 (Scheme 1). The reaction kinetics between Pd(*N*,*N*′)Cl_2 and 8-quinolinol (HQ) was examined spectrophotometrically. The reaction is first order in Pd(II) complex as k_{obs}-values are almost constant when all variants are constant except the complex concentration. The k_{obs}-values (Table 1) and the linear plots for the k_{obs} versus $[HQ]_0$ (Figs. 3 and 4) indicate the reaction is first order in HQ. The slope of the plot is the second order rate constant (k_2) of the reaction. The presence of a defined intercept (k_0) indicates the existence of a minor solvent assisted path to the overall reaction products (MeCN is a coordinating solvent).

The rate increases with a rise in temperature, as expected from the Eyring equation. Activation parameters, standard enthalpy of activation ($\Delta^{\ddagger}H^{\circ}$) and standard entropy of activation ($\Delta^{\ddagger}S^{\circ}$) were calculated from Eyring plots (Figs. 5 and 6) and are recorded in Table 2. The $\Delta^{\ddagger}H^{\circ}$ value is actually the sum of the $\Delta^{\ddagger}H^{\circ}$ value for the reaction (for the pre-equilibrium step) and the $\Delta^{\ddagger}H^{\circ}$ value for the second Cl^- displacement. The same is true for the $\Delta^{\ddagger}S^{\circ}$ value also. The activation parameter values corroborate with the experimental k_2-values. The order for $\Delta^{\ddagger}H^{\circ}$ and $\Delta^{\ddagger}S^{\circ}$ are: Pd(NaiEt)Cl_2 > Pd(NaiMe)Cl_2 > Pd(NaiBz)Cl_2 and Pd-(α-NaiR) > Pd(β-NaiR). The iso-kinetic plot (Fig. 7) supports an identical mechanism for the reaction of Pd(*N*,*N*′)Cl_2 with HQ. Kinetic studies in the presence of

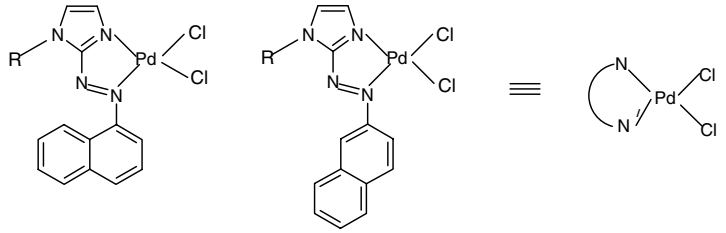

Pd(α-NaiR)Cl_2 (**1**) Pd(β-NaiR)Cl_2 (**2**) Pd(N,N′)Cl_2

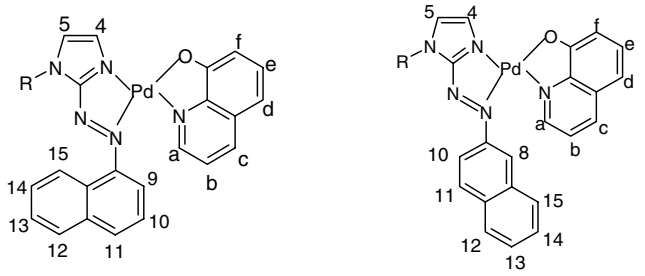

R = Me (**a**), Et (**b**), CH_2Ph (**c**)

[Pd(α-NaiR)(Q)][ClO_4) (**3**) [Pd(β- NaiR)(Q)][ClO_4) (**4**)

Scheme 1.

Table 1
Pseudo-first-order rate constants (k_{obs}) for reactions of 8-quinolinol with Pd(R′aiR)Cl_2 in MeCN at 298 K

Pd(R′aiR)Cl_2	10^3 [HQ]$_0$ (mol dm^{-3})	10^3 k_{obs} (s^{-1})	10 k_2 (dm^3 mol^{-1} s^{-1})	10^3 k_0 (s^{-1})
Pd(α-NaiMe)Cl_2 (**1a**)	1.0	0.51	2.30	0.29
	3.0	0.99		
	5.0	1.45		
	7.0	1.90		
	10.0	2.59		
Pd(α-NaiEt)Cl_2 (**1b**)	1.0	0.48	1.94	0.28
	3.0	0.86		
	5.0	1.25		
	7.0	1.64		
	10.0	2.22		
Pd(α-NaiBz)Cl_2 (**1c**)	1.0	0.57	3.45	0.23
	3.0	1.27		
	5.0	1.97		
	7.0	2.67		
	10.0	3.70		
Pd(β-NaiMe)Cl_2 (**2a**)	1.0	0.62	4.27	0.19
	3.0	1.46		
	5.0	2.32		
	7.0	3.20		
	10.0	4.45		
Pd(β-NaiEt)Cl_2 (**2b**)	1.0	0.58	3.91	0.18
	3.0	1.36		
	5.0	2.12		
	7.0	2.92		
	10.0	4.10		
Pd(β-NaiBz)Cl_2 (**2c**)	1.0	0.67	5.22	0.14
	3.0	1.71		
	5.0	2.73		
	7.0	3.80		
	10.0	5.37		

[Pd(R′aiR)Cl_2]$_0$ = 1.00×10^{-4} mol dm^{-3}.

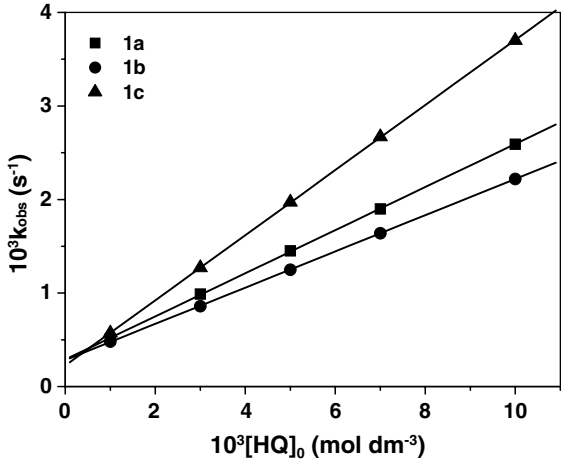

Fig. 3. Plots of k_{obs} vs. [HQ]$_0$ for the reactions: Pd(α-NaiR)Cl_2 + HQ in MeCN. [Pd(α-NaiR)Cl_2]$_0$ = 1.00×10^{-4} mol dm^{-3} at 298 K.

externally added Cl^-(LiCl) reveal that the rate as well as k_{obs} decreases inversely with [Cl^-]$_0$ (Table 3), which supports the mechanism given in Scheme 2. The dissociation

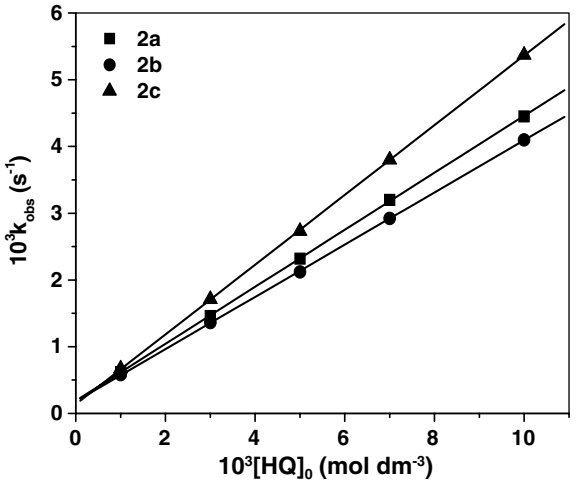

Fig. 4. Plots of k_{obs} vs. [HQ]$_0$ for the reactions: Pd(β-NaiR)Cl_2 + HQ in MeCN. [Pd(β-NaiR)Cl_2]$_0$ = 1.00×10^{-4} mol dm^{-3} at 298 K.

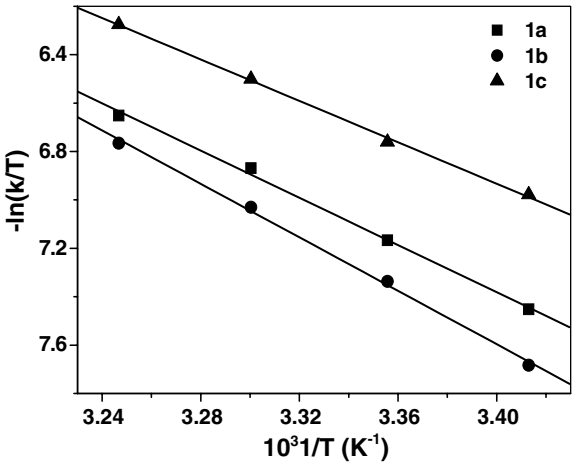

Fig. 5. Plots of ln(k/T) vs. ($1/T$) for the reactions: Pd(α-NaiR)Cl_2 + HQ in MeCN.

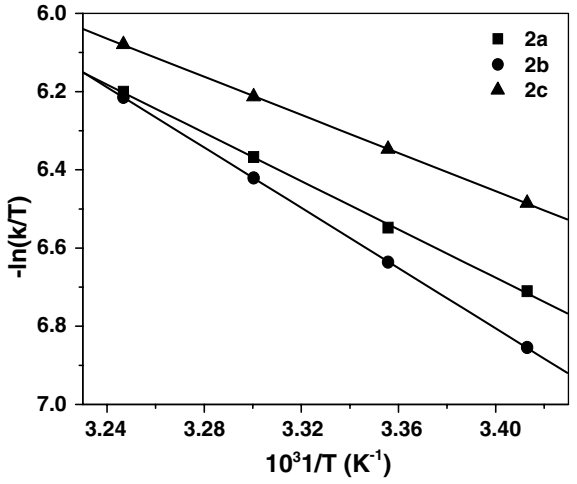

Fig. 6. Plots of ln(k/T) vs. ($1/T$) for the reactions: Pd(β-NaiR)Cl_2 + HQ in MeCN.

Table 2
Second order rate constants (k_2) at different temperatures and activation parameters of the reactions

Pd(R′aiR)Cl_2	Temperature (K)	$10 \times k$ ($dm^3\ mol^{-1}\ s^{-1}$)	$\Delta^{\ddagger}H^{\circ}$ (kJ mol^{-1})	$\Delta^{\ddagger}S^{\circ}$ (J K^{-1} mol^{-1})
Pd(α-NaiMe)Cl_2 (**1a**)	293	1.70	41(±5)	−121(±23)
	298	2.30		
	303	3.15		
	308	3.98		
Pd(α-NaiEt)Cl_2 (**1b**)	293	1.35	46(±5)	−105(±21)
	298	1.42		
	303	2.68		
	308	3.55		
Pd(α-NaiBz)Cl_2 (**1c**)	293	2.73	36(±3)	−134(±15)
	298	3.58		
	303	4.55		
	308	5.80		
Pd(β-NaiMe)Cl_2 (**2a**)	293	3.57	26(±2)	−166(±8)
	298	4.37		
	303	5.20		
	308	6.25		
Pd(β-NaiEt)Cl_2 (**2b**)	293	3.42	32(±3)	−145(±12)
	298	3.95		
	303	5.47		
	308	6.01		
Pd(β-NaiBz)Cl_2 (**2c**)	293	3.71	20(±2)	−182(±15)
	298	5.26		
	303	6.12		
	308	7.05		

of the second Pd–Cl bond is the rate controlling process and the dissociation of the first Pd–Cl bond is affected by externally added Cl^- ion. The product was isolated and characterized as [Pd(*N*,*N*′)(Q)]ClO_4. The nucleophilic substitution process involves direct displacement of 2 Cl^- ions by 8-quinolinol (Eq. (1)). In the acetonitrile medium, HQ will exist largely in the undissociated form [23].

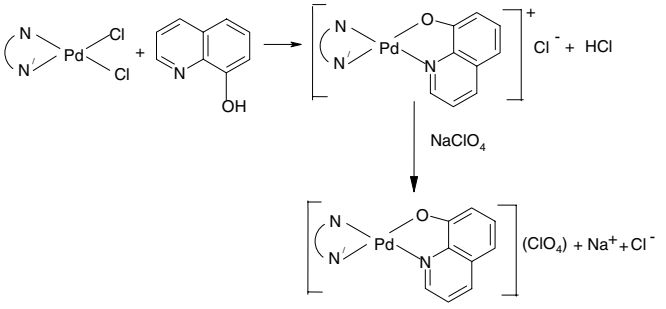

(1)

The observed rate is

$$\text{Rate} = \{k_0 + k_2[\text{HQ}]_0\}[\text{Pd(R′aiR)Cl}_2] = k_{\text{obs}}[\text{Pd(R′aiR)Cl}_2]$$

(where $k_2 = \frac{kK1}{[\text{Cl}^-]_0}$ = constant at constant $[\text{Cl}^-]_0$ and $k_{\text{obs}} = k_0 + k_2[\text{HQ}]_0$). The k_0 and k_2 are the intercept and the slope of the plot of k_{obs} versus $[\text{HQ}]_0$ respectively. The nucleophile is a undissociated N,OH donor ligand. It is probable that the highly negative O donor will coordinate first with the positively charged metal center, with fast dissociation

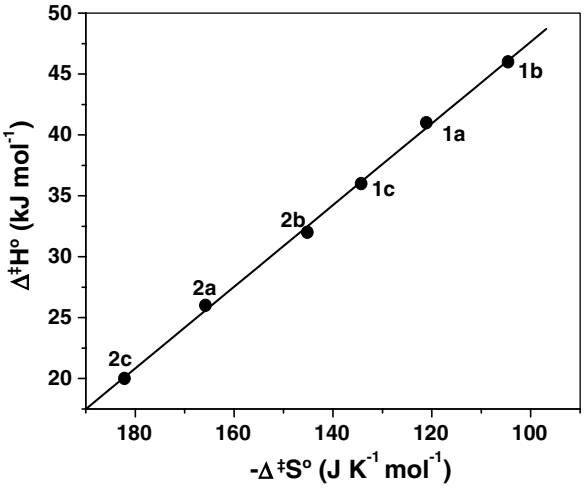

Fig. 7. Plot of $\Delta^{\ddagger}H^{\circ}$ vs. $\Delta^{\ddagger}S^{\circ}$ i.e. iso-kinetic plot for the reactions: Pd(R′aiR)Cl_2 + HQ in MeCN.

Table 3
Effect of externally added LiCl on the pseudo-first-order rate constants (k_{obs}) for reactions of 8-quinolinol with Pd(R′aiR)Cl_2 in MeCN at 298 K

Pd(R′aiR)Cl_2	10^3 $[\text{LiCl}]_0$ (mol dm^{-3})	$10^3 \times k_{\text{obs}}$ (s^{-1})
Pd(α-NaiMe)Cl_2 (**1a**)	0.2	1.38
	0.4	0.75
	0.6	0.53
	0.8	0.42
	1.0	0.34
Pd(α-NaiEt)Cl_2 (**1b**)	0.2	1.19
	0.4	0.67
	0.6	0.50
	0.8	0.41
	1.0	0.35
Pd(α-NaiBz)Cl_2 (**1c**)	0.2	1.89
	0.4	0.88
	0.6	0.60
	0.8	0.43
	1.0	0.33
Pd(β-NaiMe)Cl_2 (**2a**)	0.2	2.22
	0.4	1.09
	0.6	0.72
	0.8	0.52
	1.0	0.39
Pd(β-NaiEt)Cl_2 (**2b**)	0.2	2.03
	0.4	0.93
	0.6	0.62
	0.8	0.40
	1.0	0.27
Pd(β-NaiBz)Cl_2 (**2c**)	0.2	2.62
	0.4	1.17
	0.6	0.73
	0.8	0.44
	1.0	0.21

$[\text{Pd(R′aiR)Cl}_2]_0 = 1.00 \times 10^{-4}$ mol dm^{-3}, $[\text{HQ}]_0 = 5.00 \times 10^{-3}$ mol dm^{-3}.

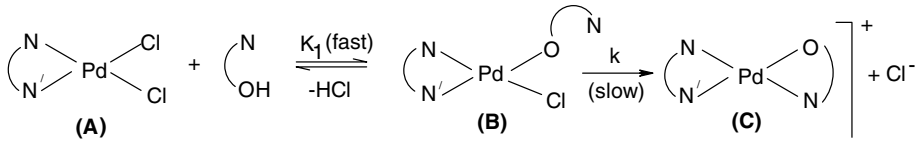

Scheme 2.

of the first Pd–Cl bond, and finally forms a stable four coordinated square planar intermediate complex (**B**). Then quinoline-N (which remains free in **B**) slowly coordinates with Pd(II) as a compulsion of chelate stability. Obviously the latter rate is slower than the former rate. Therefore the second Pd–Cl bond cleavage is the rate-determining step. This is also supported by the effect of externally added Cl^- ions (LiCl). A plausible mechanism is given in Scheme 2. There are two parallel pathways: one is the existence of a minor solvent assisted path where MeCN substitutes Cl^- initially, then MeCN is displaced by HQ and finally forms the reaction product (**C**) (Scheme 3). Although the steric crowding of the α-/β-naphthyl group in the N,N' chelating ligand is significant, its electron withdrawing property, due to conjugation, stabilizes the Pd(N,N') chelated species in preference to de-chelation.

The kinetic data in Table 1 reveal that the magnitude of k increases in the order Pd(α-NaiEt)Cl_2 < Pd(α-NaiMe)Cl_2 < Pd(α-NaiBz)Cl_2. This is because the electron withdrawing tendency of the Bz group is greater than Me, which in turn is slightly greater than Et.

3.2. Product characterization

To a MeCN solution of the complex Pd(N,N')Cl_2, HQ was added and the orange colored solution was stirred for about 24 h. It was filtered and allowed to evaporate almost to dryness at room temperature. The mass so produced was then dissolved in MeOH and $NaClO_4$ (aq) was added. A brown precipitate formed which was filtered and then washed with water and cold MeCN. The dried product was chromatographed over silica gel and MeCN eluted an orange-red band. Finally the dried product was characterized by micro-analytical data (experimental section), UV–Vis, IR. (Table 4) and ^{1}H NMR (Table 5) spectral data. The molar conductance data in MeCN solution (Λ_M = 75–90 S cm^2 mol^{-1}) show a 1:1 electrolytic nature of the complexes. The IR spectra of the complexes display a sharp stretch at 1360–1375 cm^{-1} which corresponds to ν(N=N) and is red shifted by 5–10 cm^{-1} from that of Pd(NaiR)Cl_2 [24]. This may be attributed to the charge delocalization from coordinated Q^- to the chelated NaiR motif. The binding is indirectly established by the disap-

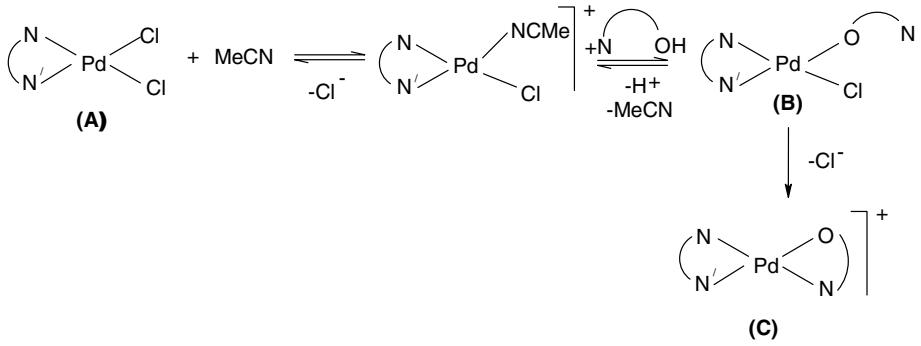

Scheme 3.

Table 4
Spectral data (FT-IR and UV–Vis) of [Pd(α/β-NaiR)(Q)](ClO$_4$)

Compounds	IR spectral data[a] (cm^{-1})			UV–Vis spectral data[b] λ_{max}, nm (ε, dm^3 mol^{-1} cm^{-1})
	ν(N=N)	ν(C=N)	ν(Pd–O)	
[Pd(α-NaiMe)(Q)](ClO$_4$) (**3a**)	1560	1651	465	393 (18730), 482 (9498)
[Pd(β-NaiMe)(Q)](ClO$_4$) (**4a**)	1558	1651	472	394(18724), 481 (9495)
[Pd(α-NaiEt)(Q)](ClO$_4$) (**3b**)	1560	1651	468	395 (18720), 485 (9500)
[Pd(β-NaiEt)(Q)](ClO$_4$) (**4b**)	1558	1651	470	394 (18718), 486 (9499)
[Pd(α-NaiBz)(Q)](ClO$_4$) (**3c**)	1559	1652	466	395 (18726), 483 (9489)
[Pd(β-NaiBz)(Q)](ClO$_4$) (**4c**)	1559	1652	469	391 (18728), 483 (9488)

[a] KBr disk.
[b] In MeCN solution.

Table 5
^{1}H NMR spectral data of [Pd(α/β-NaiR)(Q)](ClO$_4$) in CD$_3$CN

Compound	δ, ppm (J, Hz)													
	4-H[i]	5-H[i]	8-H[i]	9-H[j]	10-H[k]	11- 13-H[k]	14-H[k]	15-H[k]	a-H[j]	b-H[k]	c-H[k]	d-H[k]	e-H[k]	f-H[j]
[Pd(α-NaiMe)(Q)](ClO$_4$) (**3a**)	7.02	6.88		7.67 (8.0)	7.52	7.40	7.35	7.46	9.65 (8.0)	9.08	8.54	8.22	8.00	8.28 (8.0)
[Pd(α-NaiEt)(Q)](ClO$_4$) (**3b**)	7.00	6.85		7.65 (8.0)	7.50	7.40	7.33	7.45	9.60 (8.0)	9.00	8.58	8.20	8.00	8.30 (8.0)
[Pd(α-NaiBz)(Q)](ClO$_4$) (**3c**)	7.10	6.95		7.72 (8.0)	7.55	7.42	7.38	7.50	9.68 (8.0)	9.10	8.60	8.25	8.05	8.34 (8.0)
[Pd(β-NaiMe)(Q)](ClO$_4$) (**4a**)	7.07	6.90	7.76		7.96	7.60	7.50	7.40	9.45 (8.0)	8.80	8.53	8.10	8.00	8.27 (8.0)
[Pd(β-NaiEt)(Q)](ClO$_4$) (**4b**)	7.04	6.85	7.80		8.00	7.58	7.50	7.45	9.40 (8.0)	8.80	8.50	8.20	8.00	8.30 (8.0)
[Pd(β-NaiBz)(Q)](ClO$_4$) (**4c**)	7.10	6.90	7.86		8.05	7.64	7.50	7.45	9.50 (8.0)	8.85	8.55	8.22	8.05	8.35 (8.0)

[i] Broad singlet.
[j] Doublet.
[k] Multiplet.

pearance of two *ν*(Pd–Cl) bands corresponding to the *cis*-$PdCl_2$ configuration [24–26] and the appearance of new bands at 1560–1570 and 480–500 cm^{-1} due to *ν*(C–O) and *ν*(Pd–O), respectively. All the complexes exhibit a structureless band at 1090–1100 cm^{-1} corresponding to *ν*(ClO_4), suggesting the lack of any significant interaction in the solid state [27].

The solution electronic spectra of the complexes were recorded in the range 900–200 nm in MeCN. The absorptions below 400 nm are due to intramolecular charge transfer and are not considered further. Two absorptions at 475–485 and 515–525 nm (Fig. 8), absent in the free ligands, may represent charge transfer transitions localized on the metallated fragment [28].

The ^{1}H NMR spectra of the complexes were recorded in CD_3CN and the data are collected in Table 5. The proton numbering pattern is shown in Scheme 1. The data reveal that the signals in the spectra of the complexes are shifted downfield relative to the free ligand values [18]. This supports the coordination of the ligand to Pd(II). An important feature of the spectra is the shifting of the imidazole protons 4-H and 5-H to lower *δ*-values, in general, relative to the naphthyl protons (6-H–13-H). The imidazole protons suffer downfield shifting by 0.1-0.2 ppm compared to the free ligand positions. This supports the strong preference of imidazole-N binding to Pd(II). The naphthyl protons appear as multiplets, except a broad singlet for 6-H and doublet for 8-H in [Pd(β-NaiR)(Q)](ClO$_4$) and a

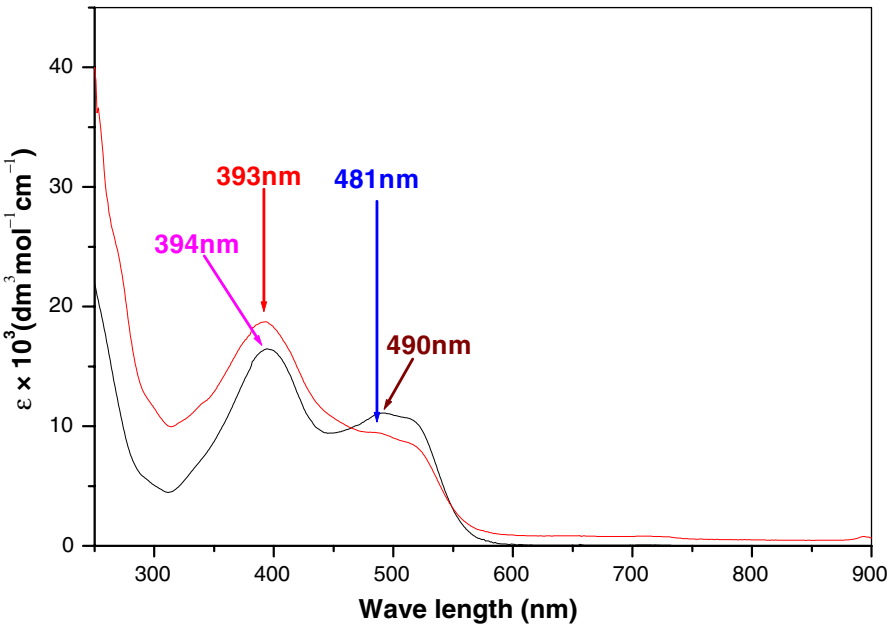

Fig. 8. UV–Vis spectra of [Pd(β-NaiMe)Cl$_2$] (black line) and [Pd(β-NaiMe)(Q)](ClO$_4$) (red line) in MeCN solution. (For interpretation of the references in color in this figure legend, the reader is referred to the web version of this article.)

doublet for 15-H in all the complexes. The 1-alkyl group appears as a singlet for 1-Me in [Pd(α/β-NaiMe)(Q)](ClO$_4$), a quartet for –N–CH$_2$– and a triplet for the –CH$_3$ group in [Pd(α/β-NaiEt)(Q)](ClO$_4$) and a singlet for –CH$_2$– and benzyl protons in the [Pd(α/β-NaiCH$_2$Ph)(Q)](ClO$_4$) complexes.

4. Conclusion

The kinetics of the reactions between Pd(*N*,*N*′)Cl$_2$ and 8-quinolinol (HQ) were examined spectrophotometrically at 500 nm under pseudo-first-order conditions in MeCN. The reactions are first order with respect to the complex and HQ. The rate of the reaction is largely influenced by the π-acidity of the chelating ligand; substitution in the naphthylazoimidazole backbone influences the rate of the substitution process significantly. Activation parameters $\Delta^{\ddagger}H^{\circ}$ and $\Delta^{\ddagger}S^{\circ}$ of the reactions were measured, which corroborates the kinetic rate data. The products isolated from the reaction between Pd(NaiR)Cl$_2$ and HQ in MeCN have been characterized by spectral data and support the composition [Pd(NaiR)(Q)](ClO$_4$).

Acknowledgements

Financial help from Jadavpur University is gratefully acknowledged. We thank Dr. C. Sinha, Professor of Chemistry, Jadavpur University for his helpful discussions.

References

[1] H. Chen, J.A. Parkinson, S. Parsons, R.A. Coxall, R.O. Gould, P.J. Sadler, J. Am. Chem. Soc. 124 (2002) 3064.
[2] A.H. Velders, H. Kooijman, A.L. Spek, J.G. Haasnoot, D. de Vos, J. Reedijk, Inorg. Chem. 39 (2000) 2966.
[3] P. Banerjee, Coord. Chem. Rev. 19 (1999) 190.
[4] B. Lippert, Coord. Chem. Rev. 18 (1999) 263.
[5] M. Kato, J. Takahashi, Y. Sugimoto, C. Kosuge, S. Kishi, S. Yano, J. Chem. Soc., Dalton Trans. (2001) 747.
[6] J. Li, L.M. Zheng, I. King, T.W. Doyle, S.H. Chan, Curr. Med. Chem. 8 (2001) 121.
[7] S.J. Lippard, in: I. Bertini, H.B. Gray, S.J. Lippard, J.S. Valentine (Eds.), Bioinorganic Chemistry, University Science Books, Mill Valley, CA, 1994, p. 505.
[8] P.D. Beer, Acc. Chem. Res. 31 (1998) 71.
[9] Y.S. Yoo, Y.S. Sohn, Y.K. Do, J. Inorg. Biochem. 73 (1999) 187.
[10] F.A. Cotton, G. Wilkinson, Advanced Inorganic Chemistry, 5th ed., John Wiley, New York, 1988.
[11] D. Das, M.K. Nayak, C. Sinha, Transition Met. Chem. 22 (1997) 172.
[12] S. Dey, M. Ray, P. Banerjee, Inorg. React. Mech. 2 (2000) 267.
[13] S. Saha, P.K. Ghosh, A. Mahapatra, Transition Met. Chem. 30 (6) (2005) 706.
[14] S. Saha, T. Majumdar, A. Mahapatra, Inorg. React. Mech. 6 (2006) 19.
[15] S. Saha, T. Majumdar, A. Mahapatra, Transition Met. Chem. 31 (2006) 1017.
[16] S. Saha, T. Majumdar, A. Mahapatra, Indian J. Chem. A 45 (2006) 877.
[17] S. Saha, P.K. Sarkar, A. Mahapatra, Transition Met. Chem. 31 (3) (2006) 389.
[18] S. Saha, A. Mahapatra, Inorg. React. Mech. 6 (2006) 71.
[19] J. Dinda, P.K. Santra, C. Sinha, L.R. Falvello, J. Organomet. Chem. 629 (2001) 28.
[20] S. Pal, D. Das, P. Chattopadhyay, C. Sinha, K. Panneerselvam, T.H. Lu, Polyhedron 19 (2000) 1263.
[21] R. Roy, T.K. Misra, C. Sinha, A. Mahapatra, A. Sanyal, Transition Met. Chem. 22 (1997) 453.
[22] R. Roy, D. Das, M. Banerjee, A. Mahapatra, Transition Met. Chem. 26 (2001) 205.
[23] T. Suganuma, A. Tanada, H. Tomizawa, M. Tanaka, E. Miki, Inorg. Chim. Acta 320 (2001) 22.
[24] J. Dinda, P.K. Santra, C. Sinha, L.R. Falvello, J. Organomet. Chem. 629 (2001) 28.
[25] C.K. Pal, S. Chattopadhyay, C. Sinha, D. Bandyopadhyay, A. Chakravorty, Polyhedron 13 (1994) 999.
[26] D. Das, M.K. Nayak, C. Sinha, Transition Met. Chem. 22 (1997) 172.
[27] S. Goswami, W. Kharmawphlang, A.K. Deb, S.M. Peng, Polyhedron 15 (1996) 3635.
[28] Y. Wakatsuki, M. Yamazaki, P.A. Grutasch, M. Santhanam, A.C. Ku, J. Am. Chem. Soc. 107 (1985) 8153.